

Wind turbine impact evolution and beam blockage analysis on the Weather Radar Network of the Meteorological Service of Catalonia

O. Argemi¹, N. Pineda¹, T. Rigo¹
A. Belmonte², X. Fabregas², J. Bech³



Oriol Argemi

¹Meteorological Service of Catalonia, Barcelona, Spain, oargemi@meteo.cat

²Signal Theory and Communication Dep., Technical University of Catalonia, Barcelona, Spain, belmonte@tsc.upc.edu

³Astronomy and Meteorology Dep., University of Barcelona, Barcelona, Spain, joan.bech@ub.edu
(Dated: 31 May 2012)

1. Introduction

The increase of windmills in the NE of Spain over the last few years has been affecting the quality of the C-Band radar data provided by the Weather Radar Network (XRAD) of the Meteorological Service of Catalonia (SMC). Different types of undesirable effects have been appearing into the radar data, basically as clutter, blockage and wrong Doppler measurements. Since 2008, the SMC in collaboration with the Signal Theory and Communication Department of the Technical University of Catalonia (UPC) have performed the wind turbine impact analysis based on the radar beam blockage, also considering the topography blockage factor which is really relevant in Catalonia (e. g. Bech et al., 2003; Trapero et al., 2009). The results reported in Belmonte and Fabregas (2010) permits examination of the signal degradation in Doppler weather radars, combining both terrain obscuration and wind turbine effects. Moreover, a specific simulation tool in three-dimensional media has been developed for this aim, which considers high resolution topography and a realistic windmill Radar Cross Section (RCS) to describe the radar beam propagation. The obtained results allow establishing windmill blockage criteria for the XRAD, with the aim of mitigating, mainly by preventing new wind farm installations that can potentially affect on the data quality.

2. Wind farm evolution and wind turbine effects in Catalonia

In Catalonia (NE of Spain), the installation of wind farms has proliferated: Wind energy reaches a total capacity of 1MW per year at the end of 2011 and the tendency is to increase this value (ICAEN, 2012).

The four C-Band Doppler radars of the XRAD are differently affected by windmills, taking into account the distances and relative heights between radars and windmills, according to the WMO recommendations (OPERA, 2006). In this regard, CDV and LMI radars are the most affected at this time and also potentially in the future, while PDA and PBE are not currently affected (see Fig.1).

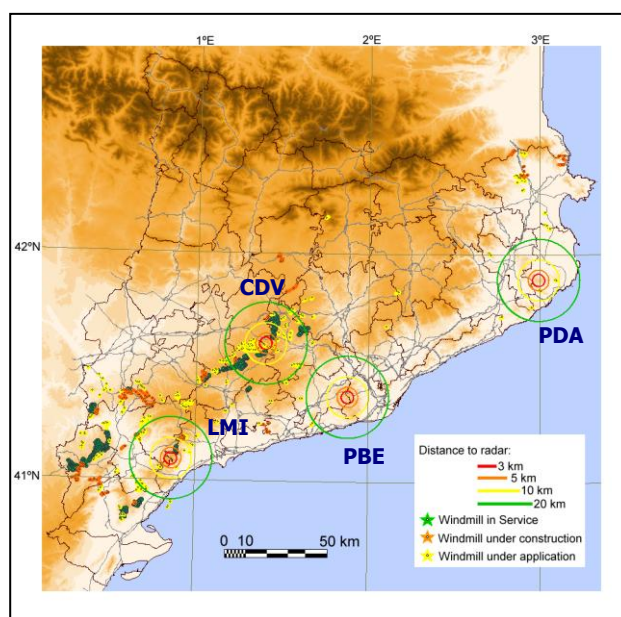


Fig. 1 Topographic map of Catalonia, showing wind turbine farms (in service, under construction or under application) and the XRAD radars (CDV, LMI, PBE and PDA).

Since 2007, undesirable wind turbine effects can be observed on the XRAD data, which basically corresponds to the three different types of common problems reported in Norin and Haase (2012): wind turbine clutter (WTC), blockage (attenuation) and erroneous Doppler measurements. All these effects are mainly remarkable in the CDV radar data (Fig. 2).

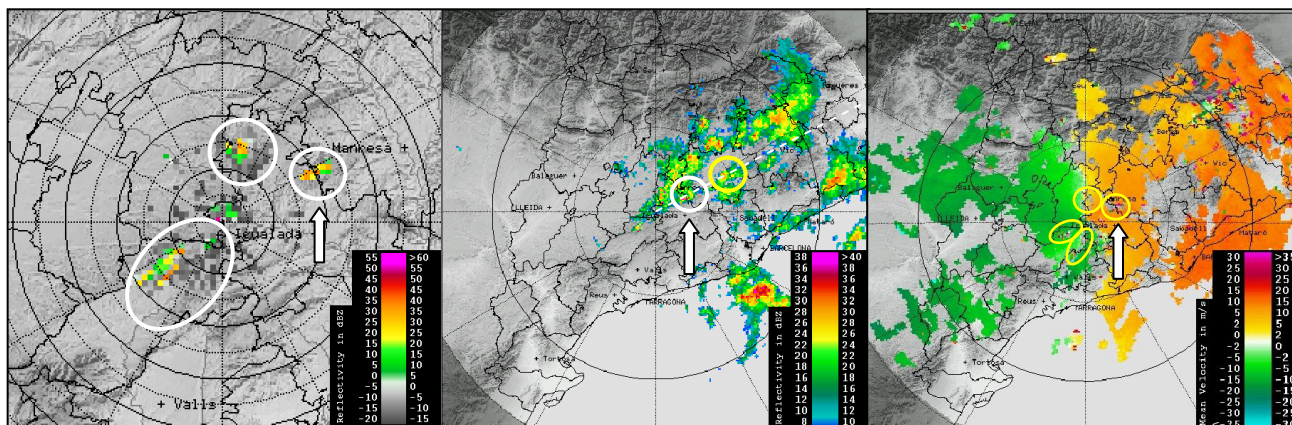


Fig.2 CDV-150km short range radar product showing reflectivity (dBZ, left and centre panels) and radial velocity field (m/s, right panel). From left to right panel: WTC, blockage and erroneous velocity; rings plotted every 5 and 50 km, respectively.

In Fig. 2, left panel shows WTC (white circles corresponding to different wind farms). Centre panel shows meteorological echoes with attenuation in the NE direction (white dashed line): a real thunderstorm (yellow circle) is attenuated due to the radar beam impact to the wind farm (white arrow), which appears as a false echo. And right panel shows bad Doppler measurements: both static errors (as holes) and dynamic errors (as noise) as described in Norin and Haase (2012). These kinds of errors appear in the wind farm locations, inside the yellow circles.

3. Beam blockage analysis:

3.1 Technique: windmill, wind farm and terrain obscuration effects

In this study we use the technique to calculate the windmill beam blockage developed by Belmonte and Fabregas (2010). It is based on the split-step solution to the parabolic wave equation describing beam propagation, and it considers a realistic windmill RCS and the terrain obscuration effects, under standard atmospheric conditions and at arbitrary transmitter and receiver configurations.

The starting up conditions for the analysis are set for the ideal case: assuming the terrain as flat earth, with the windmill exactly in the centre of the radar line of sight (RLS) and perpendicular to the blades plane, i.e. in the worst case position which maximises the area of the wind turbine seen by the radar (see Fig. 3). In this case, the blockage should be computed as the maximum possible attenuation (energy losses) by the relative windmill RCS as a function of range.

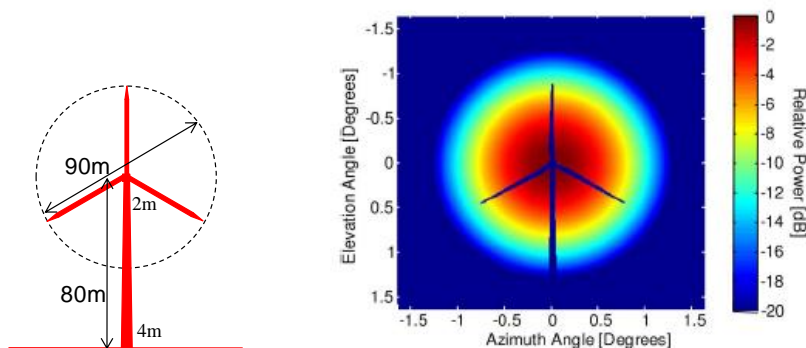


Fig. 3 Left panel: the considered as standard windmill features; Right panel: the Gaussian radiation diagram (for the case of an antenna of 1.2° horizontal and 1.1° vertical beam width) with the windmill RCS. The range is 3 km.

The approach described above allows for a simple description of the effect of a single wind turbine on the beam radar cross section. This approach can be generalized to a wind farm or group of turbines by considering the effect of two wind

turbines aligned, one behind the other like people in a queue, but supposing 1 km of distance between them. In this situation, the worst position evaluated is when the first windmill is indeed in the RLS but the second one has an azimuth off-axis angle of 0.4° . Fig. 4 shows the results: first row panels obtained with the single wind turbine, and second row panels for the wind farm scenario. In a symmetric way, relative power and truncation losses are computed for turbines located up to 1 km away from the radar. Right panels show the total losses (blue lines), taking into account both, windmill or wind farm truncation losses, respectively, and terrain truncation losses versus the wind turbine range.

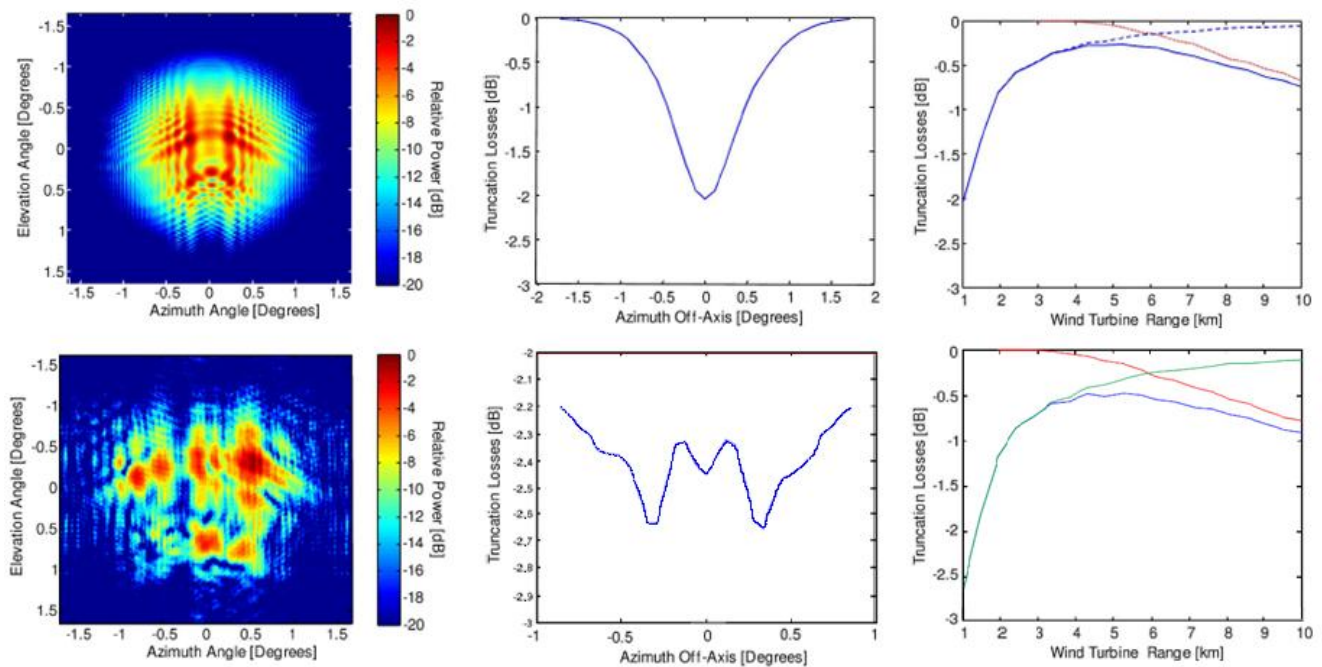


Fig. 4 Upper row panels correspond to the losses computed by the windmill; lower row corresponds to a wind farm. The left panels show the radiation diagram after the blockage; middle panels show losses versus azimuth relative to the beam centre; right figures show losses versus range (solid blue line: total losses; red line: terrain losses; dashed blue and green line: windmill and wind farm obscuration losses).

3.2 Applying beam blockage technique to a real case (XRAD)

The beam blockage analysis for the XRAD has considered current wind farm locations (see Fig. 1) and specific radar features needed to simulate properly the beam propagation (see Table 1). Moreover, the procedure considers a high topography resolution (15 m) by using a digital elevation model (DEM).

Radars		Geographical coordinates			Antenna features		
Name	Site-name	Lat ($^\circ$)	Lon ($^\circ$)	Height (m)	BW H ($^\circ$)	BW V ($^\circ$)	Frequency (GHz)
Panadella	CDV	41.601	1.402	825	1.20	1.10	5.632
Tivissa_Llaberia	LMI	41.090	0.863	923	1.20	1.10	5.610
Puig d'Arques	PDA	41.888	2.997	542	1.20	1.10	5.625
Vallirana	PBE	41.373	1.881	630	1.58	1.85	5.648

Table 1 Radar features (XRAD).

4. Results: XRAD analysis

Taking into account the actual wind farms installed, there are mainly two radars affected by windmills at current time: CDV and LMI. Regarding the DEM and the radar features, the first results (Fig. 5) show that the CDV radar should be the most affected, specially because there are two wind farms in the RLS at distances lower than 10 km (left panel). On the other hand, closest wind turbines to the LMI radar (right panel) have elevations much lower than the radar antenna, and, in the standard atmospheric conditions, they are below the RLS. Thus, in this case their blockage is nearly negligible.

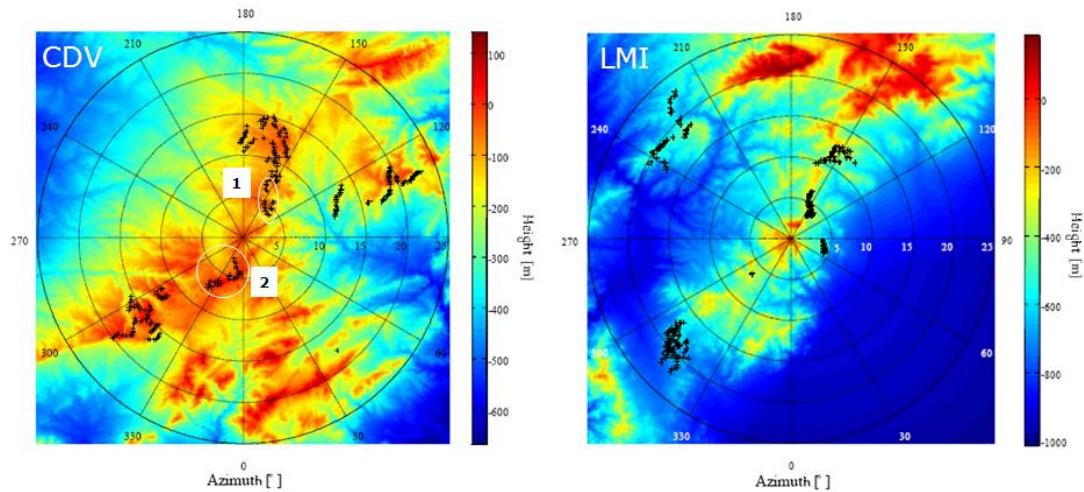


Fig 5 Relative height of terrain versus azimuth in a range of 25 km. Zero height means the radar reference. In black crosses, the current operative windmills. The numbers 1 and 2 (left panel) correspond to the more problematic wind farms currently installed: 1) 'Turó del Magre', located in the NE direction (around 150° of azimuth); 2) 'Montargull', located in the SW direction (around 330-360° of azimuth)

After a complete analysis, the 'Montargull' wind farm presents the major blockage impact in the CDV data. In this work, it is shown the beam blockage analysis results for the azimuth range of (300, 360)°, which includes the effects of this wind farm.

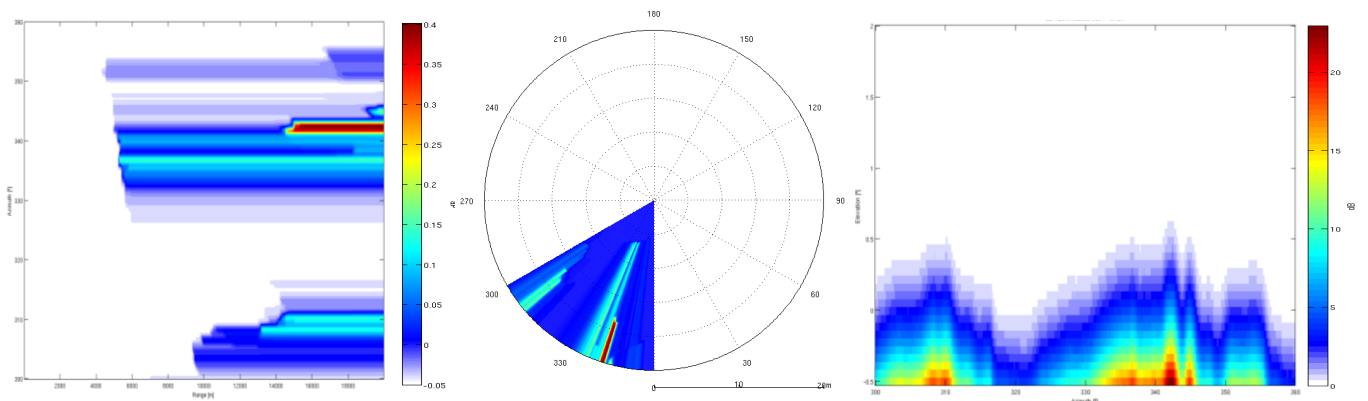


Fig 6 Terrain losses (dB). Left panel: versus range (m) and azimuth (°) in Cartesian coordinates; centre panel: versus range (km) and azimuth (°) in polar coordinates; right panel: versus azimuth (°) and elevation (°). Total range: 20 km.

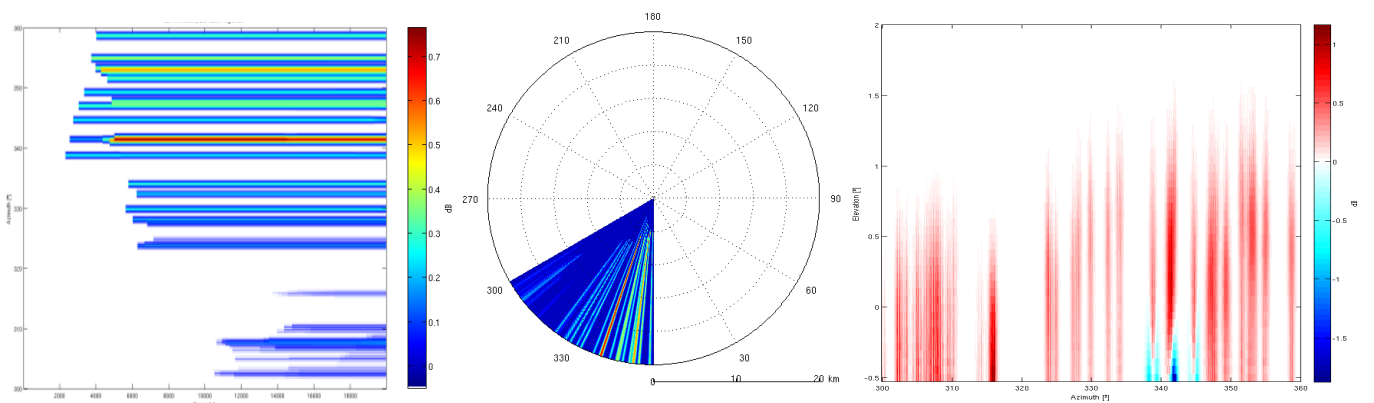


Fig 7 Windmill losses (dB). Left panel: versus range (m) and azimuth (°) in Cartesian coordinates; centre panel: versus range (km) and azimuth (°) in polar coordinates; right panel: versus azimuth (°) and elevation (°). Total range: 20 km.

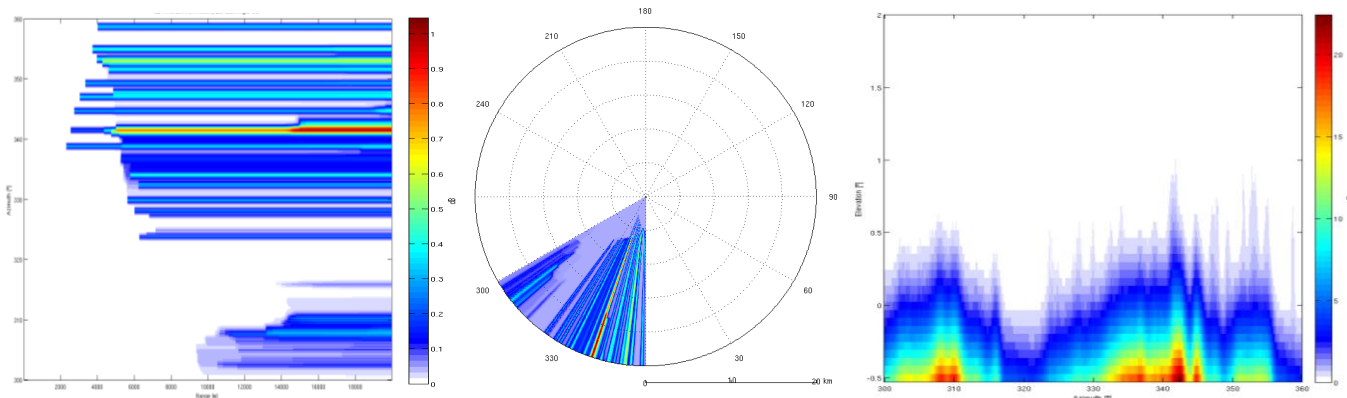


Fig 7 Total losses (dB). Left panel: versus range (m) and azimuth (°) in Cartesian coordinates; centre panel: versus range (km) and azimuth (°) in polar coordinates; right panel: versus azimuth (°) and elevation (°). Total range: 20 km.

Fig. 6 and Fig. 7 show the energy losses (dB) due to terrain and windmills blockage, respectively, computed in a separate way. Both losses have been calculated in an elevation range from -0.5° up to 2° , and for a maximum range of 20 km. Nevertheless, the lower elevation task of the radar is at 0.6° and the vertical beam width is 1.2° . It has to be taken into account for the

Finally, total losses are shown in Fig. 8. For example, the azimuth of 341.5° is the direction (Fig. 9) that presents more blockages. Thus, considering this azimuth, the respective local losses and the cumulative total losses in this direction can be calculated.

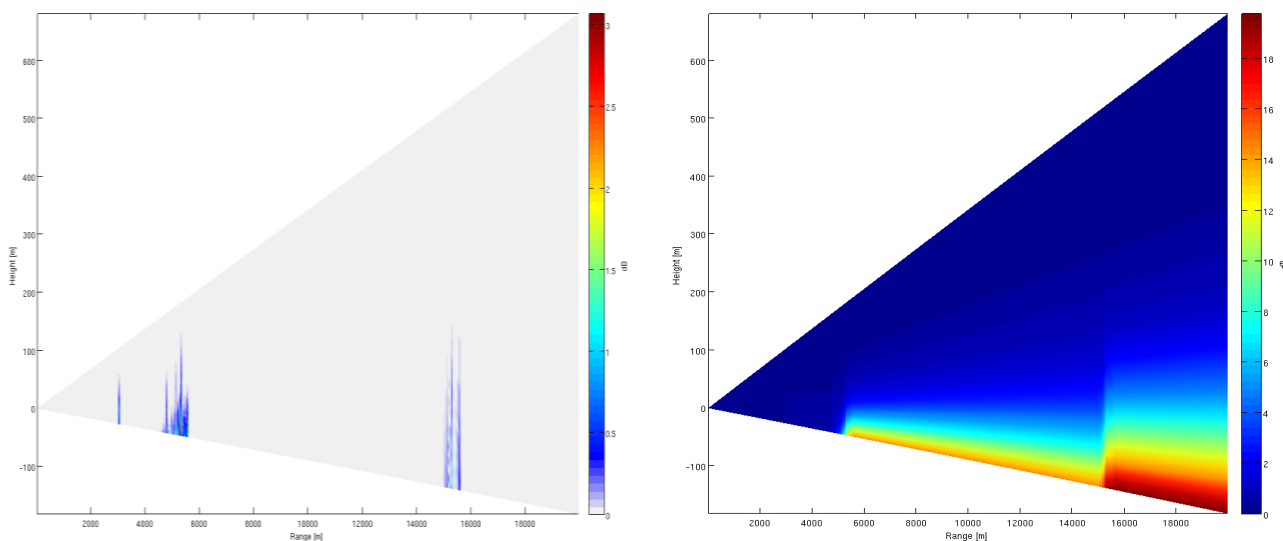


Fig 9 Energy losses (dB), height (m) versus range (m), in the azimuth of 341.5° . Left panel: local losses; right panel: cumulative losses.

In general, looking at the results shown in this section, a similar behavior as reported previously in section 3 can be observed: for closest distances to the radar, up to 3-5 km, the major blockage contribution is done by windmills, while, for wind turbine ranges beyond the 5 km mark, terrain obscuration term wins in relevance and turbine truncation can be adequately neglected.

5. Mitigation efforts and conclusions

At SMC, mitigation efforts have focused to analyze current blockage impact from the already installed wind farms, and to generate a self guidance statement based on blockage criteria (Table 2). Moreover, distinct advancements in measurement capabilities to quantify and evaluate radar beam blockages have been performed with the possibility to simulate new realistic scenarios. Therefore, self recommendations can be made to the autonomous government in order to prevent new wind farm installations in the radar surrounding areas.

Zone	A	B	C	D	E
Range (km)	0-3	3-5	5-10	10-20	> 20
Attenuation in case of beam impact (dB)	> 0.5	< 2.5	< 0.5	< 0.1	~ 0.0
Probability of WTC	Yes	Yes	Yes	Yes	Yes
Probable affectation	High	Moderate	Low	Very low	Negligible

Table 2 Blockage criteria

Results from section 4, and previous analysis, have lead to establish distance thresholds at the values of 3, 5, 10 and 20 km. These thresholds allow defining and distinguishing five different impact zones (A, B, C, D and E) in the criteria (see Table 2), where each zone has attenuation values associated in case of wind turbines in the radar line of sight. For example, a beam impact taking place in the A zone, up to 3 km, the attenuation must reach values above (or not less than) 0.5 dB, while in the B zone must be below 2.5 dB, in the C zone below 0.5 dB and so on. In this regard, there is a reference scale of probable affectation. Nevertheless, if the windmill size increases the attenuation should be greater.

In general, the blockage impact tends to decrease exponentially with the distance, similar as in Vogt et al. (2011), but the final beam blockage for a particular case depends not only on the distance but also on the terrain surface and the windmill shape and size, as it is shown in this study. This conclusion leads to the fact that a simulation tool may be essential for deciding the reliability of radar measurements affected by blockage, or even the suitability of wind turbine locations.

References

- Bech J., Codina B., Lorente J., Bebbington D., 2003: *The sensitivity of single polarization weather radar beam blockage correction to variability in the vertical refractivity gradient*. J Atmos Ocean Technol (20) 845-855, [http://dx.doi.org/doi:10.1175/1520-0426\(2003\)020%3C0845:TSOSPW%3E2.0.CO;2](http://dx.doi.org/doi:10.1175/1520-0426(2003)020%3C0845:TSOSPW%3E2.0.CO;2)
- Belmonte A., Fàbregas X., 2010: *Analysis of Wind Turbines Blockage on Doppler Weather Radar Beams*, IEEE Antennas and Wireless Propagation Letters, Vol. 9.
- ICAEN, 2012. Wind Energy Data Base. Energy Catalan Institute, ICAEN, <http://www20.gencat.cat/portal/site/icaen>
- Norin L., Haase G., 2012: *Doppler Weather Radars and Wind Turbines*. In *Doppler Radar Observations* (J Bech and JL Chau, ed.). InTech, Rijeka, Croatia. pp. 333-354, <http://dx.doi.org/10.5772/39029>
- OPERA, 2006: *Impact of Wind Turbines on Weather Radars*, OPERA II programme WP 1.8.
- Trapero L., Bech J., Rigo T., Pineda N., Forcadell D., 2009: *Uncertainty of precipitation estimates in convective events by the Meteorological Service of Catalonia radar network*. Atmos. Res., 93, 408-418, <http://dx.doi.org/doi:10.1016/j.atmosres.2009.01.021>
- Vogt R. J., Crum T. D., Greenwood W., Ciardi E. J., Guenther R., March 2011: *Recent Canges to NOAA's wind turbine impact evaluation process and mitigation efforts*. NOAA's National Weather Service, Norman, Oklahoma.